Transition States for the [2 + 2] Addition of CH_2=CH_2, CH_2=O, and [M]=O across the C=C Double Bond of Ketene: Electronic Structure and Energy Decomposition

Dirk V. Deubel*

Department of Chemistry, University of Calgary, Calgary, Alberta, Canada T2N 1N4[1]

Received: August 29, 2001; In Final Form: November 1, 2001

Organic molecules with double bonds, such as ethylene and formaldehyde, are well-known to undergo [2 + 2] cycloadditions across the C=C moiety of ketene. Surprisingly, the same pathway was recently predicted to be kinetically favored in the reaction of $CpReO_3$ with ketene, in contrast to the additions of other metal oxides to the heterocumulene. Since the origin of the activation energies of [2 + 2] cycloadditions was poorly understood, a comparative density-functional study on the [2 + 2] addition of X=Y (CH_2=CH_2, CH_2=O, and CpO_2Re=O) across the C=C bond of ketene has been carried out. The electronic structure of the transition states has been analyzed in terms of interactions between the ketene and X=Y fragments. The analysis reveals that, besides stabilizing orbital interactions, additional contributions such as electrostatics and repulsion due to the Pauli principle determine the activation energies of cycloadditions. The stabilization arising from orbital interactions is weakest in the transition state for the metal−oxide addition to the heterocumulene, although this reaction has the lowest activation barrier.

Introduction

The concepts developed by Woodward and Hoffmann to classify pericyclic reactions belong to the tools of every chemist.[2] However, simple cycloadditions that are of considerable industrial importance[3] challenge these concepts: the thermal [2 + 2] additions of ketenophiles such as ethylene[4] and formaldehyde[5] across the C=C moiety of ketene.[6] Whether a [$2\pi_s + 2\pi_a$] topology (Figure 1, left) or a [$2\pi_s + (2\pi_s + 2\pi_s)$] topology[7] involving the C=O moiety of ketene (Figure 1, right) describes the transition states (TS) best has controversially been discussed.[8,9] Theoretically predicted transition structures[4,5] and a recent frontier-orbital study[8,10] on the reactions give evidence for the latter topology model. Common fragment-based charge- and energy-decomposition schemes[11,12] have not yet been used to analyze these reactions. These methods[11,12] characterize molecules of the type A−B in terms of interactions between the fragments A and B,[13] and they should become valuable tools of organic chemists to gain insight into the electronic structure of transition states for cycloadditions.

Tremendous research efforts focus on transition-metal−oxide additions across unsaturated carbon−carbon bonds,[14] since there is a considerable industrial interest in the activation of double bonds by readily accessible metal oxides, beyond the common methods for cis dihydroxylation using osmium tetraoxide and permanganate.[3] Several density-functional studies on these reactions were recently reported because their mechanisms provide some academic challenges.[15−23] While transition-metal−oxide additions to ethylene follow a [3 + 2] pathway only,[15−24] cyclopentadienyltrioxorhenium(VII)[25] kinetically favors the [2 + 2] addition across the C=C bond of ketene.[26] The [3 + 2] activation energies can easily be predicted from frontier-orbital analysis[21,22] or even from thermochemical data using Marcus theory.[23] However, in our recent computational study, we were unable to rationalize the activation energies of [2 + 2] additions.[22]

* Corresponding author. E-mail: deubel@ucalgary.ca.

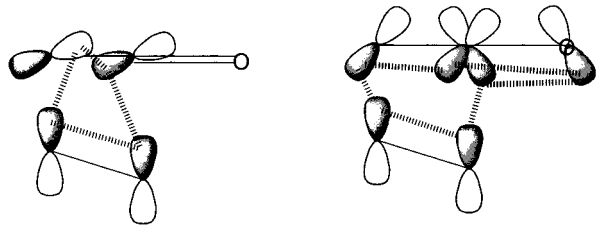

Figure 1. Suggested models for the topology of the transition state for the [2 + 2] addition of ethylene to ketene.

We have performed a comparative density-functional (DFT) study on the electronic structure of the transition states for the addition of X=Y (CH_2=CH_2, CH_2=O, and $CpReO_3$) across the C=C moiety of ketene. We use two state-of-the-art decomposition schemes based on the interactions between the X=Y and ketene fragments in the TS: charge decomposition analysis (CDA)[11] and the Extended Transition State (ETS) method.[12]

Methods

Geometry Optimization and Energy Calculation. The molecules and transition states were optimized at the gradient-corrected DFT level using the exchange functional of Becke[27] and the correlation functional of Perdew[28] (BP86). Relativistic effects were considered using the zeroth-order regular approximation (ZORA).[29] Uncontracted Slater-type orbitals (STOs) were used as basis functions for the SCF calculations.[30] The basis functions at the metal have triple-ζ quality, augmented with a set of 6p functions. The basis set at the other atoms has double-ζ quality, augmented with a set of d-type polarization functions. The $(1s)^2$ core electrons of C and O and the $(1s2s2p3s3p3d4s4p4d)^{46}$ inner shells of Re were treated within the frozen-core approximation.[31] An auxiliary basis set of s, p, d, f, and g STOs was utilized to fit the molecular densities and

10.1021/jp0133440 CCC: $22.00
Published on Web 12/15/2001

to represent the Coulomb and exchange potentials in each SCF cycle.[32] This basis-set combination is denoted III∼.[22,23] Unless otherwise stated, energies reported refer to the BP86/III∼ level. The calculations were carried out using the ADF 2000 program package.[34]

Electronic-Structure Analysis. For the calculation of atomic partial charges, the NPA method[35] was employed. Donor−acceptor interactions in the transition states were examined using charge decomposition analysis (CDA).[11] CDA was developed as a quantum-chemical interpretation of the Dewar−Chatt−Duncanson model,[36] and it has mainly been applied to transition-metal complexes.[37] The use of CDA for the analysis of olefin epoxidations was recently discovered.[38] The Kohn−Sham MOs of a transition state are expressed as a linear combination of the MOs of the fragments ketene (denoted donor) and X═Y (CH_2═CH_2, CH_2═O, and CpO_2Re═O, denoted acceptor) in the geometry of the TS. We define (i) the interaction among the occupied orbitals of ketene and the vacant orbitals of X═Y as donation *d*, (ii) the interaction among the occupied orbitals of X═Y and the vacant ketene orbitals as back-donation *b*, (iii) the interaction of the occupied orbitals of both fragments as repulsive polarization *r*, and (iv) the interaction of the vacant orbitals of both fragments as rest term Δ. This term will be approximately zero if the reaction is thermally symmetry-allowed. The CDA calculations were carried out with Gaussian 98 package[39] and the CDA 2.1 program[40] using basis set II.[41] Energy decomposition of the TS was studied with the extended transition state method (ETS).[12] The transition structures are again divided into the two fragments ketene and X═Y. The activation energy ΔE is the sum of the two contributions strain energy ΔE_{str} and interaction energy ΔE_{int} ($\Delta E = \Delta E_{str} + \Delta E_{int}$). Strain energy ΔE_{str} is the difference between the energy of the isolated fragments in the TS geometry and their energy in the equilibrium geometry. ΔE_{int}, which is the energy of interaction between the fragments in the TS geometry, can in turn be partitioned into three components ($\Delta E_{int} = \Delta E_{elst} + \Delta E_{Pauli} + \Delta E_{orb}$). ΔE_{elst} gives the electrostatic interaction energy between the fragments, which is calculated with a frozen electron-density distribution in the TS geometry. Pauli repulsion (ΔE_{Pauli}) considers the energy required for antisymmetrization and renormalization of the Kohn−Sham orbitals of the superimposing ketene and X═Y fragments. ΔE_{Pauli} represents the repulsive interaction energy between the fragments which is caused by the fact that two electrons with the same spin cannot occupy the same region in space (Pauli principle). Finally, the stabilizing orbital-interaction term ΔE_{orb} is calculated with the Kohn−Sham orbitals relaxing to their optimal form.

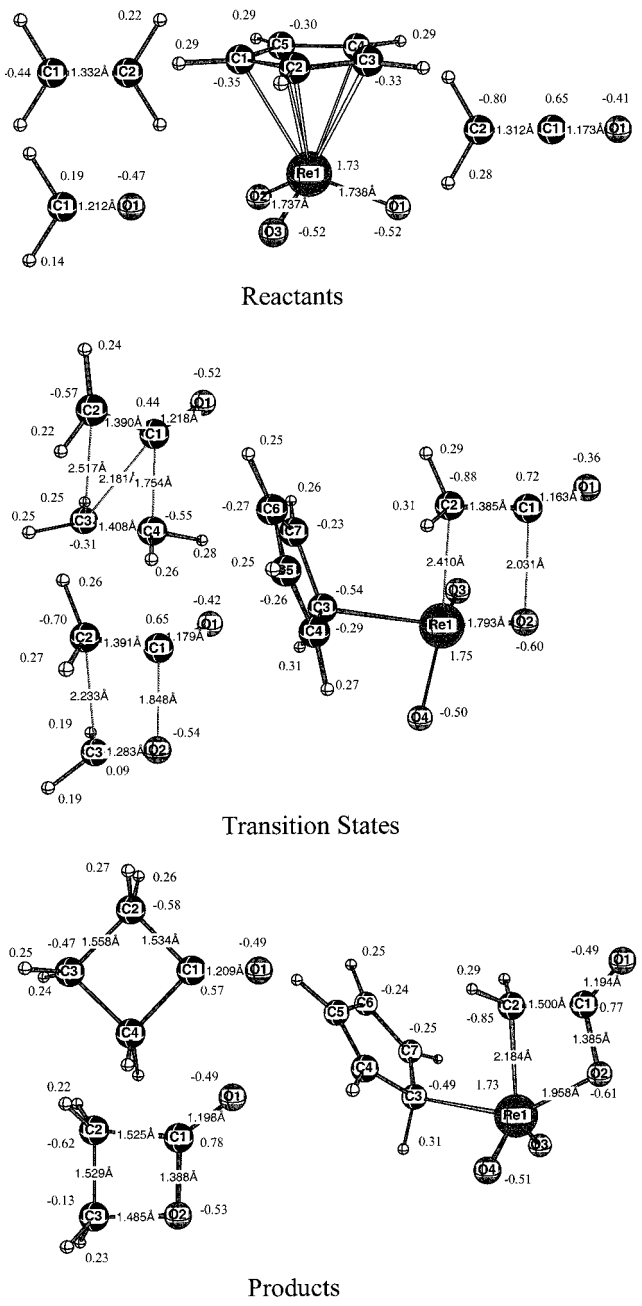

Figure 2. Optimized geometries (BP86/III∼) of the reactants, transition states and products for the [2 + 2] addition of X═Y (CH_2═CH_2, CH_2═O, and CpO_2Re═O) across the C═C moiety of ketene. Calculated NPA atomic charges.

Results and Discussion

Structures and Energies. The optimized geometries of the reactants and transition states for the [2 + 2] additions of CH_2═CH_2, CH_2═O, and CpO_2Re═O across the C═C moiety of ketene are shown in Figure 2. Additional structural data are provided in Table 1. We focus on a brief comparison of the three transition structures, since the reactions were already separately studied using quantum-chemical methods, and geometries in good agreement with the results of the current work were predicted.[4,5,22] The transition-state geometry for the reaction of ethylene indicates a highly asynchronous reaction with the C4−C1 bond to the central carbon of ketene being formed first. It is interesting to note that the C1−C3 distance in the TS is much shorter than the C2−C3 distance, although a bond will be formed between the latter two atoms during the reaction. The C1−O1 bond is elongated compared to this distance in free ketene, in the product, and in the other TS. Ketene is strongly bent in the "carbenoid-like"[4a] transition structure for ethylene addition; the O1−C1−C2 angle is 135.8° (Table 1), and the C2 and O1 atoms are significantly twisted out of the C3−C4−C1 plane; we calculate a C3−C4−C1−C2 dihedral angle of 61.4° (Table 1). The transition-state geometry for the reaction of formaldehyde is similar to the TS for the ethylene addition. The ketene moiety is less deformed and the C2−C3 distance is shorter than that in the former reaction. The TS structure for the [2 + 2] addition of $CpReO_3$ across the C═C moiety shown in Figure 2 corresponds to the reaction with the lowest activation energy with regard to peri-, chemo-, stereo-, and regioselectivity. The Cp ligand changes its coordination mode from η^5 in the reactant to η^1 in the TS and in the product.[42] Compared to the reaction of CH_2O with ketene, the C1−O2 distance is longer (Figure 2). The ketene moiety is less bent and less twisted than

TABLE 1: Calculated Structural Parameters in the Transition States for the [2 + 2] Additions of X=Y (CH_2=CH_2, CH_2=O, and CpO_2Re=O) Across the C=C Moiety of Ketene (H_2C2=C1=O1): C1−Y and C2-X Distances (Å), O1−C1−C2 Angles (deg), and X−Y−C1−C2 Torsion Angles (deg)[a]

X=Y	C1−Y	C2−X	O1−C1−C2	X−Y−C1−C2	ΔE	ΔE_r
CH_2=CH_2	1.754	2.517	135.8	61.4	22.4	−21.8
CH_2=O	1.848	2.234	147.5	49.4	17.9	−31.7
CpO_2Re=O	2.031	2.410	157.8	39.3	6.7	−10.9

[a] Activation barriers ΔE and reaction energies ΔE_r (kcal/mol).

TABLE 2: Charge Decomposition Analysis (CDA) Results of the Transition States[a]

	d (ketene→X=Y)		*b* (ketene←X=Y)				
X=Y	value	main contrib.	value	main contrib.	*d*/*b*	*r* (ket. ↔ X=Y)	Δ
CH_2=CH_2	0.181	HOMO → LUMO	0.318	LUMO ← HOMO	0.57	−0.589	0.054
CH_2=O	0.214	HOMO → LUMO	0.223	LUMO ← HOMO-1	0.96	−0.409	0.042
CpO_2Re=O	0.394	HOMO → LUMO	0.171	LUMO ← HOMO-2	2.32	−0.432	0.038

[a] Donation *d* (ketene → X=Y), backdonation *b* (ketene ← X=Y), repulsive polarization *r* (ketene ↔ X=Y), and rest term Δ.

TABLE 3: Sum of NPA Atomic Partial Charges (e) in the Reactants and in the Transition States

	reactants				transition states				differences (TS-reactant)			
	X=Y		ketene		X=Y		ketene		X=Y		ketene	
X=Y	X	Y	CH_2	CO	X	Y	CH_2	CO	X	Y	CH_2	CO
CH_2=CH_2	0.00	0.00	−0.25	0.25	0.23	−0.01	−0.09	−0.13	0.23	−0.01	0.16	−0.38
CH_2=O	0.52	−0.52	−0.25	0.25	0.54	−0.62	−0.18	0.26	0.02	−0.10	0.07	0.01
CpO_2Re=O	0.59	−0.59	−0.25	0.25	0.64	−0.70	−0.31	0.37	0.06	−0.11	−0.06	0.12

in the other two reactions (Table 1). The structures of the reaction products are also given in Figure 2. In the products of the formaldehyde and $CpReO_3$ addition, the C1−O2 distances are comparably short due to conjugation with the exocyclic carbonyl group.

The calculated activation barriers and reaction energies are also listed in Table 1. For the addition of ethylene and formaldehyde to ketene, activation energies of 22.4 and 17.9 kcal/mol, respectively, are predicted at the BP86 DFT level. The calculated activation energies are slightly smaller than the barriers calculated using the DFT−Hartree−Fock hybrid method B3LYP, the ab initio method MP2, and experimental data.[8,43] The [2 + 2] addition of $CpReO_3$ is the reaction with the lowest activation barrier (6.7 kcal/mol). The three cycloadditions are clearly exothermic (Table 1), justifying electronic-structure analyses of the transition states referring to the reactants rather than to the products.[44] In contradiction to the Bell−Evans−Polanyi principle,[45] the fastest reaction has the smallest thermodynamic driving force.

Charge Decomposition Analysis (CDA). Donor and acceptor interactions in the transition states have been analyzed using charge decomposition analysis (CDA), which was developed by Dapprich and Frenking;[11] the results are given in Table 2. The rest terms Δ, which refer to the interactions between the vacant orbitals of the X=Y and ketene fragments, are close to 0, indicating that the three transition states can properly be described in terms of donor−acceptor interactions between the fragments and that the reactions are thermally symmetry-allowed. Ketene is arbitrarily denoted donor, and X=Y is denoted acceptor. The analysis reveals that back-donation *b* from occupied ethylene orbitals to vacant ketene orbitals provides the predominant contribution in the TS for the ethylene addition. Donation *d* from ketene to ethylene is significantly less pronounced; the *d*/*b* ratio is 0.57. In contrast, both contributions are of same importance in the transition state of the formaldehyde addition (*d*/*b* = 0.96, Table 2). In the TS for the addition of $CpReO_3$, the orbital interactions are reverse (*d*/*b* = 2.32); i.e., electrons have mainly flowed from ketene to the metal oxide. The comparison of the CDA results for the three transition states indicate a fundamental change in the mechanism. There is no inherent connection between the three reactions other than the superficial formalism that they are all [2 + 2] cycloadditions. Note that this finding is reflected by the transition structures (Figure 2).

The information provided by CDA is only partially accessible from calculated NPA atomic charges (Table 3, Figure 2). The charges in the TS of the ethylene addition also indicate an electron flow to the ketene fragment. For the other two reactions, a slight charge transfer from ketene to X=Y is predicted (Table 3). The carbene-like addition of the heterocumulene to ethylene is corroborated by the atomic charges in the TS: There is a more negative charge at the oxygen and a less negative charge at C2 of ketene in comparison to the reactant (Figure 2). However, attempts to localize zwitterionic cyclopropane derivatives as stationary points on the BP86/III∼ potential energy surface have not been successful.

A configuration analysis of the [2 + 2] addition of ethylene to ketene leads to results that are comparable to the *d*/*b* value in CDA: charge transfer from ethylene to ketene in the TS is double as large than the reverse charge transfer.[8] The analysis along the intrinsic reaction path (IRC)[46] showed that both interactions synchronously increase during the reaction, approaching the TS.[8] For the other two reactions, a configuration analysis has not been reported.[8] The CDA results advise caution not to extend the conclusions drawn from the reaction of ethylene with ketene to the addition of other ketenophiles to the heterocumulene.

A key feature of CDA is to provide insight into the frontier orbitals involved in the interactions. A plot of the predominant orbitals of the reactants is given in Figure 3; the corresponding energy levels are listed in Table 4. The involved frontier-orbitals of formaldehyde (HOMO-1, LUMO) are lower in energy than the corresponding ethylene orbitals (HOMO, LUMO), elucidating the increase of donation *d* from the heterocumulene in the TS for formaldehyde addition compared to ethylene addition (Table 2). From formaldehyde to the metal oxide, there is a further decrease of the LUMO energy. The HOMO-2 of $CpReO_3$, which is most important in back-donation, has about

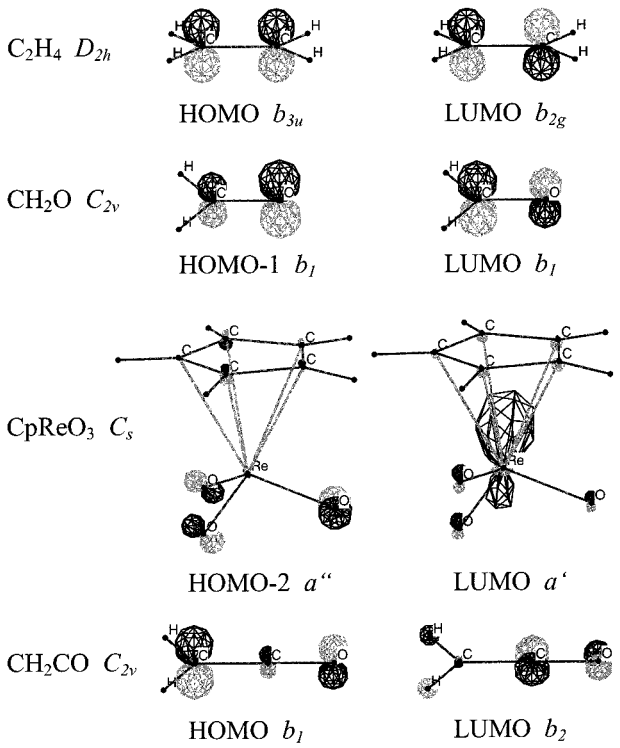

Figure 3. Plots of the predominant frontier orbitals of the reactants.

TABLE 4: Energies ϵ (eV) of the Frontier Orbitals of X═Y Being Predominant in CDA[a]

		d (ketene→X═Y)			*b* (ketene←X═Y)		
X═Y	symm.	orbital	Γ	ϵ	orbital	Γ	ϵ
CH_2═CH_2	D_{2h}	LUMO	b_{2g}	−1.34	HOMO	b_{3u}	−7.15
CH_2═O	C_{2v}	LUMO	b_1	−2.93	HOMO-1	b_1	−10.32
CpO_2Re═O	C_s	LUMO	a'	−3.72	HOMO-2	a''	−7.38

[a] Frontier-orbital energies of ketene (C_{2v}): HOMO (b_1) −6.37, LUMO (b_2) −2.65.

the same energy as the ethylene HOMO. Note that there is only a very small contribution from metal orbitals to the HOMO-2 of $CpReO_3$ (Figure 3). Back-donation from the $CpReO_3$ HOMO-2 to the ketene LUMO is therefore less important than from the C_2H_4 HOMO to the acceptor orbital of the heterocumulene.

Even though the structures of the reactants and the product pretend that the carbonyl group does not participate in the [2 + 2] cycloaddition of ethylene to ketene, the analysis reveals that the classical [$2\pi_s + 2\pi_a$] model with the C═O moiety as a noninvolved bystander is wrong (Figure 1). Not only steric reasons, i.e., a free access to the central carbon of the heterocumulene, but also stereoelectronic reasons due to the presence of the carbonyl moiety enable ketenes to undergo [2 + 2] cycloadditions. Since the formation of the second C−C bond proceeds at a large extent of reaction, the alternative [$2\pi_s + (2\pi_s + 2\pi_s)$] model also does not appropriately describe the nature of the transition state. The initial orbital interaction between the ethylene HOMO and the ketene LUMO, which is the π^* orbital of the C═O bond, is predominant in the transition state. In the TS for the reactions of formaldehyde and $CpReO_3$ with ketene, the LUMO of the heterocumulene is also involved but to a lesser extent.

Extended Transition State Analysis (ETS). The information about how strongly orbital interactions in the TS influence the activation energy is not provided by the CDA results reported in the previous section. For gaining insight into the origin of reactivity, the extended transition state (ETS) method has been employed, which was developed by Ziegler and Rauk.[12] The results of this energy-decomposition scheme are listed in Table 5 and visualized in Figure 4.

First, the reactants must be deformed out of their equilibrium structure to their geometry in the transition state; the corresponding energy is denoted deformation or strain energy ΔE_{str}. ΔE_{str} can separately be evaluated for each fragment, i.e., X═Y and ketene; it is the difference between the energy of the isolated fragment in the TS geometry and the energy of its equilibrium structure. While there is a slight deformation of the ethylene and formaldehyde fragments, the rhenium oxide both requires an elongation of the Re═O bond and a change in the configuration of the other ligands at the metal. The strain energy for the metal−oxide fragment is therefore comparably large (see ΔE_{str}(X═Y) values in Figure 4b). A huge strain energy ΔE_{str}(ketene) of the ketene fragment is necessary to reach the TS of ethylene addition. For the other reactions, the deformation energy of the ketene fragment is smaller, as expected from the larger calculated O1−C1−C2 angles in the transition states (Table 1). The large total strain energy ΔE_{str}(total) for the ethylene addition (37.5 kcal/mol), which is the sum of ΔE_{str}(X═Y) and ΔE_{str}(ketene), might elucidate the high activation energies ΔE of the reaction (22.4 kcal/mol). However, the total strain energy in the metal−oxide addition (28.1 kcal/mol) is larger than that in the formaldehyde addition (23.6 kcal/mol), although the relative height of the activation barriers is reverse (6.7 and 17.9 kcal/mol, respectively).

The other contribution to the activation energy ΔE is the energy of interaction ΔE_{int} between the two fragments in the TS. ΔE_{int} can in turn be divided into three contributions ($\Delta E_{int} = \Delta E_{elst} + \Delta E_{Pauli} + \Delta E_{orb}$). ΔE_{Pauli} represents the repulsive interaction energy between the fragments which is caused by the fact that two electrons with the same spin cannot occupy the same region in space (Pauli principle). ΔE_{elst} is the electrostatic interaction and ΔE_{orb} gives the stabilizing orbital interactions. The results for the three transition states are very interesting (Figure 4a). Pauli repulsion is largest in the TS for ethylene addition. In the same reaction, the stabilization due to orbital interactions is also largest, which leads to a considerable interaction energy of −15.1 kcal/mol. The transition state for the formaldehyde addition to ketene scarcely benefits from the interaction between the fragments ($\Delta E_{int} = -5.8$ kcal/mol). In contrast, there is a large stabilization of the TS for $CpReO_3$ (−21.4 kcal/mol). It is remarkable that this stabilization arises from electrostatics ΔE_{elst} rather than from orbital interactions (Figure 4a). The sum of ΔE_{str} and ΔE_{int} yields the activation barrier ΔE (Figure 4b). A moderate total activation strain and

TABLE 5: Extended Transition State (ETS) Results of the Transition States. Activation Strain ΔE_{str}, Electrostatic Interaction Energy ΔE_{elst}, Pauli Repulsion ΔE_{Pauli}, Orbital Interaction Energy ΔE_{orb}, Interaction Energy $\Delta E_{int} = \Delta E_{Pauli} + \Delta E_{elst} + \Delta E_{orb}$, and Activation Energy $\Delta E = \Delta E_{str} + \Delta E_{int}$ (kcal/mol)

X═Y	ΔE_{str} (X═Y)	ΔE_{str} (ketene)	ΔE_{str} (total)	ΔE_{elst}	ΔE_{Pauli}	ΔE_{orb}	ΔE_{int}	ΔE
CH_2═CH_2	8.3	29.3	37.5	−90.0	203.4	−128.5	−15.1	22.4
CH_2═O	5.5	18.1	23.6	−74.2	152.6	−84.2	−5.8	17.9
CpO_2Re═O	14.9	13.2	28.1	−113.2	174.0	−82.2	−21.4	6.7

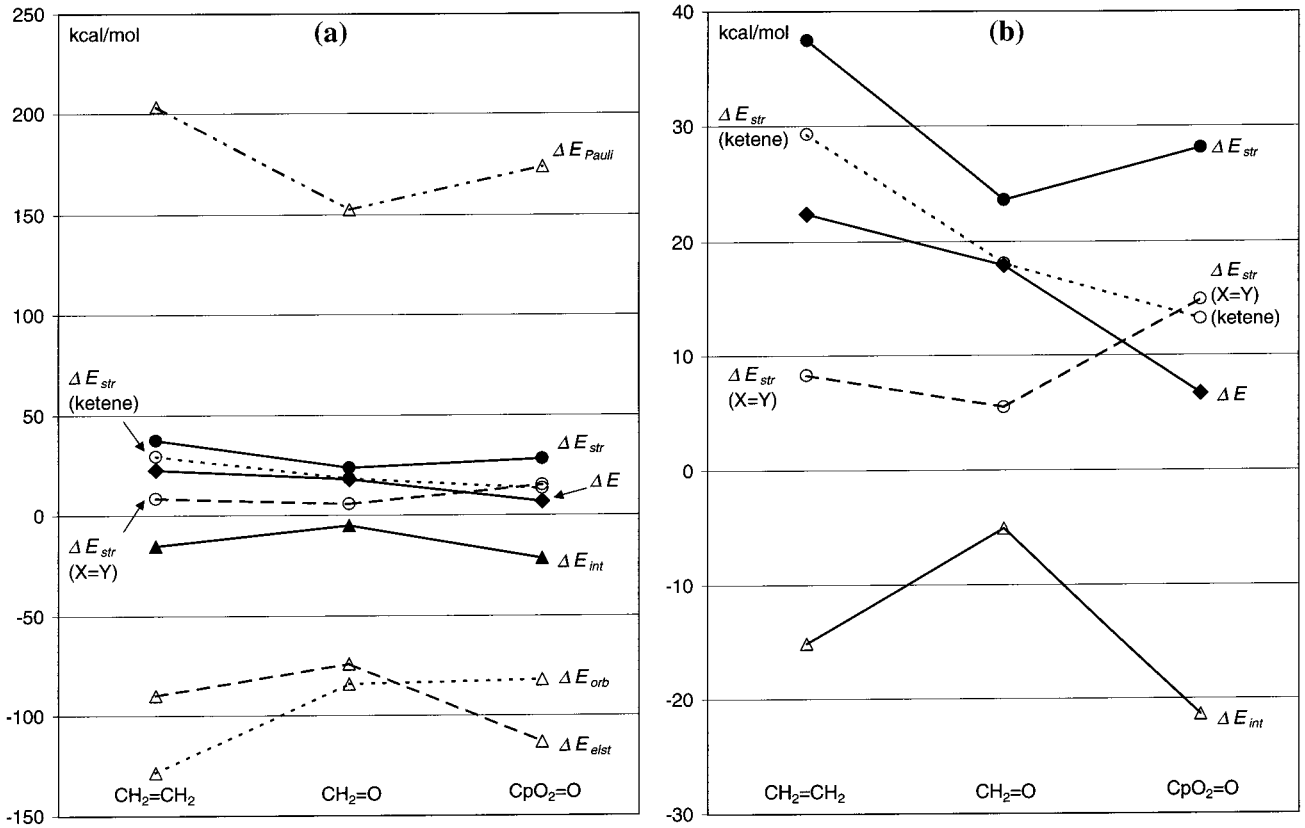

Figure 4. ETS results of the transition states. A larger scale is used in Figure 4b.

a large electrostatic stabilization in the TS elucidate the low activation barrier predicted for the metal−oxide addition.

Conclusions

(i) A complete rationalization of the activation barriers of cycloadditions is not always provided by traditional quantum-chemical concepts such as orbital energies of the reactants and calculated atomic charges. Fragment-based charge- and energy-decomposition schemes give additional insight into the origin of reactivity.

(ii) The dominant orbital interactions in the transition states for the [2 + 2] reactions of ketene with X=Y (CH_2=CH_2, H_2C=O, and CpO_2Re=O) are different. Ketene is arbitrarily denoted donor and X=Y is denoted acceptor. Back-donation *b* from the ethylene HOMO into the LUMO of the strongly bent ketene is the predominant orbital interaction in the TS for the ethylene addition. In contrast, donation *d* from the ketene HOMO into vacant orbitals of $CpReO_3$ are more important than *b* in the transition state for the metal oxide, while *d* and *b* are of equal strength in the TS for the formaldehyde addition.

(iii) The classical [$2\pi_s + 2\pi_a$] model for the topology of the transition state for the ethylene addition to ketene, which suggests that the carbonyl moiety is a noninvolved bystander in the reaction, is wrong. A better description is provided by a [$2\pi_s + (2\pi_s + 2\pi_s)$] topology, although neither model accurately considers the predominant orbital interactions in the transition state. In the [2 + 2] addition of formaldehyde and $CpReO_3$ across the C=C bond of ketene, the ketene LUMO is also significantly involved. Not only steric reasons, i.e., a free access to the central carbon of the heterocumulene, but also stereoelectronic reasons due to the presence of the carbonyl moiety allow ketenes to undergo [2 + 2] cycloadditions.

(iv) Orbital interactions provide only one of several factors that determine the activation barriers of cycloadditions. For instance, the stabilization energy arising from orbital interactions is weakest in the transition state for the $CpReO_3$ addition to the heterocumulene, although this reaction is predicted to be fastest. The transition state of this reaction is significantly stabilized by electrostatic interactions. Due to the results of this study, we are systematically investigating the transition states of other cycloadditions.

Acknowledgment. The author thanks Prof. Dr. Gernot Frenking, Dr. Sabine Schlecht, Dr. F. Matthias Bickelhaupt, Prof. Dr. Kevin P. Gable, and Prof. Dr. Kurt Dehnicke for helpful discussions. He gratefully acknowledges support by Prof. Dr. Gernot Frenking and Prof. Dr. Tom Ziegler. The author thanks the Alexander-von-Humboldt Foundation (Feodor-Lynen fellowship), the Fonds der Chemischen Industrie (Kekulé scholarship) and the Deutscher Akademischer Austauschdienst (NATO fellowship).

References and Notes

(1) URL: http://staff-www.uni-marburg.de/~deubel.

(2) Woodward, R. B.; Hoffmann, R. *The Conservation of Orbital Symmetry*; Verlag Chemie: Weinheim, Germany, 1970.

(3) (a) Wittcoff, H. A.; Reuben, B. G. *Industrial Organic Chemicals*; Wiley: New York, 1996. (b) Weissermel, K.; Arpe, H.-J. *Industrial Organic Chemistry*; Wiley-VCH: Weinheim, 3rd ed., 1997.

(4) (a) Wang, X.; Houk, K. N. *J. Am. Chem. Soc.* **1990**, *112*, 1754. (b) Bernardi, F.; Bottoni, A.; Robb, M. A.; Venturini, A. *J. Am. Chem. Soc.* **1990**, *112*, 2106. References cited therein.

(5) (a) Lecea, B.; Arietta, A.; Roa, G.; Ugalde, J. M.; Cossío, F. P. *J. Am. Chem. Soc.* **1994**, *116*, 9613. (b) Pons, J. M.; Oblin, M.; Pommier, A.; Rajzmann, M.; Liotard, D. *J. Am. Chem. Soc.* **1997**, *119*, 3333. References cited therein.

(6) (a) Staudinger, H. *Die Ketene*, Enke: Stuttgart, 1912. (b) Tidwell, T. T. *Acc. Chem. Res.* **1990**, *23*, 273.

(7) (a) Zimmermann, H. E. In *Pericyclic Reactions*; Marchand, A. P., Lehr, R. E., Eds.; Academic Press: New York, 1977; Vol. 1. (b) Pasto, D. J. *J. Am. Chem. Soc.* **1979**, *101*, 37.

(8) Yamabe, S.; Kuwata, K.; Minato, T. *Theor. Chem. Acc.* **1999**, *102*, 139.

(9) Additional models for the transition state were proposed, which focus on the predominant orbital interactions rather than on the topology of the TS: (a) Ghosez, L.; O'Donnell, M. J. In *Pericyclic Reactions*; Marchand, A. P., Lehr, R. E., Eds.; Academic Press: New York, 1977; Vol. 2. (b) Yamabe, S.; Minato, T.; Osamura, Y. *Chem. Commun.* **1993**, 450.

(10) For selected articles and textbooks, see: (a) Fukui, K. *Theory of Orientation and Stereoselection*; Springer: Berlin, 1970. (b) Sustmann, R. *Tetrahedron Lett.* **1971**, *29*, 2717. (c) Sustmann, R. *Tetrahedron Lett.* **1971**, *29*, 2721. (d) Houk, K. N. *J. Am. Chem. Soc.* **1973**, *95*, 4092. (e) Houk, K. N. *Acc. Chem. Res.* **1975**, *8*, 361. (f) Sauer, J.; Schubert, R. *Angew. Chem., Int. Ed.* **1980**, *19*, 779. (g) Nelson, D. W.; Gypser, A.; Ho, P. T.; Kolb, H. C.; Kondo, T.; Kwong, H.-L.; McGrath, D. V.; Rubin, A. E.; Norrby, P.-O.; Gable, K. P.; Sharpless, K. B. *J. Am. Chem. Soc.* **1997**, *119*, 1840. (h) Gothelf, K. V.; Jørgensen, K. A. *Chem. Rev.* **1998**, *98*, 863.

(11) Dapprich, S.; Frenking, G. *J. Phys. Chem.* **1995**, *99*, 9352.

(12) (a) Ziegler, T.; Rauk, A. *Theor. Chim. Acta* **1977**, *46*, 1. (b) Ziegler, T.; Rauk, A. *Inorg. Chem.* **1979**, *18*, 1558. (c) Ziegler, T.; Rauk, A. *Inorg. Chem.* **1979**, *18*, 1755.

(13) For recent examples, see: (a) Fonseca Guerra, C.; Bickelhaupt, F. M.; Snijders, J. G.; Baerends, E. J. *J. Am. Chem. Soc.* **2000**, *122*, 4117. (b) Diefenbach, A.; Bickelhaupt, F. M.; Frenking, G. *J. Am. Chem. Soc.* **2000**, *122*, 6449. (c) Uddin, J.; Frenking, G. *J. Am. Chem. Soc.* **2001**, *123*, 1683.

(14) For recent experimental contributions, see: (a) Döbler, C.; Mehltretter, G. M.; Sundermeier, U.; Beller, M. *J. Am. Chem. Soc.* **2000**, *122*, 10289. (b) Che, C. M.; Yu, W. Y.; Chan, P. M.; Cheng, W. C.; Peng, S. M.; Lau, K. C.; Li, W. K. *J. Am. Chem. Soc.* **2000**, *122*, 11380. (c) Wirth, T. *Angew. Chem., Int. Ed. Engl.* **2000**, *39*, 334. (d) Jonsson, S. Y.; Färnegårdh, K.; Bäckvall, J.-E. *J. Am. Chem. Soc.* **2001**, *123*, 1365. (e) Severeyns, A.; De Vos, D. E.; Fiermans, L.; Verpoort, F.; Grobet, P. J.; Jabbs, P. A. *Angew. Chem., Int. Ed. Engl.* **2001**, *40*, 586.

(15) (a) Pidun, U.; Boehme, C.; Frenking, G. *Angew. Chem.* **1996**, *108*, 3008; *Angew. Chem., Int. Ed. Engl.* **1996**, *35*, 2817. (b) Dapprich, S.; Ujaque, G.; Maseras, F.; Lledós, A.; Musaev, D. G.; Morokuma, K. *J. Am. Chem. Soc.* **1996**, *118*, 11660. (c) Torrent, M.; Deng, L.; Duran, M.; Sola, M.; Ziegler, T. *Organometallics* **1997**, *16*, 13. (d) Del Monte, A. J.; Haller, J.; Houk, K. N.; Sharpless, K. B.; Singleton, D. A.; Strassner, T.; Thomas, A. A. *J. Am. Chem. Soc.* **1997**, *119*, 9907.

(16) (a) Ujaque, G.; Maseras, F.; Lledós, A. *J. Am. Chem. Soc.* **1999**, *121*, 1317. (b) Norrby, P.-O.; Rasmussen, T.; Haller, J.; Strassner, T.; Houk, K. N. *J. Am. Chem. Soc.* **1999**, *121*, 10186. (c) Moitessier, N.; Maigret, B.; Chretien, F.; Chapleur, Y. *Eur. J. Org. Chem.* **2000**, 995.

(17) Pietsch, M. A.; Russo, T. V.; Murphy, R. B.; Martin, R. L.; Rappé, A. K. *Organometallics* **1998**, *17*, 2716.

(18) Monteyne, K.; Ziegler, T. *Organometallics* **1998**, *17*, 5901.

(19) (a) Torrent, M.; Deng, L.; Ziegler, T. *Inorg. Chem.* **1998**, *37*, 1307. (b) Torrent, M.; Deng, L.; Duran, M.; Sola, M.; Ziegler, T. *Can. J. Chem.* **1999**, *77*, 1476.

(20) (a) Houk, K. N.; Strassner, T. *J. Org. Chem.* **1999**, *64*, 800. (b) Strassner, T.; Busold, M. *J. Org. Chem.* **2001**, *66*, 672.

(21) Deubel, D. V.; Frenking, G. *J. Am. Chem. Soc.* **1999**, *121*, 2021.

(22) Deubel, D. V.; Schlecht, S.; Frenking, G. *J. Am. Chem. Soc.* **2001**, *123*, 10085.

(23) Gisdakis, P.; Rösch, N. *J. Am. Chem. Soc.* **2001**, *123*, 697.

(24) A computational study supports [2 + 2] additions of SO_3 to ethylene: Haller, J.; Beno, B. R.; Houk, K. N. *J. Am. Chem. Soc.* **1998**, *120*, 6468.

(25) (a) Romão, C. C.; Kühn, F. E.; Herrmann, W. A. *Chem. Rev.* **1997**, *97*, 3197. (b) Gable, K. P. *Advances in Organomet. Chem.* **1997**, *41*, 127. (c) Herrmann, W. A.; Kühn, F. E. *Acc. Chem. Res.* **1997**, *30*, 169.

(26) In contrast, metal-oxide additions to diphenylketene probably follow a stepwise mechanism via a zwitterionic intermediate, the cyclization of which yields the product that is thermodynamically most stable. In the reactions of $CpReO_3$ and Cp^*ReO_3 with the heterocumulene, the thermodynamically favored metallacycle is the metalla-2,5-dioxolane-3-one. For details, see ref 22 and refs cited therein. For experimental work, see: (a) Herrmann, W. A.; Küsthardt, U.; Ziegler, M. L.; Zahn, T. *Angew. Chem., Int. Ed. Engl.* **1985**, *24*, 860. (b) Herrmann, W. A.; Küsthardt, U.; Schäfer, A.; Herdtweck, E. *Angew. Chem., Int. Ed. Engl.* **1986**, *25*, 817. (c) Küsthardt, U.; Herrmann, W. A.; Ziegler, M. L.; Zahn, T.; Nuber, B. *J. Organomet. Chem.* **1986**, *311*, 163. (d) Herrmann, W. A.; Roesky, P. W.; Scherer, W.; Kleine, M. *Organometallics* **1994**, *13*, 4536.

(27) Becke, A. D. *Phys. Rev. A* **1988**, *38*, 3098.

(28) Perdew, J. P. *Phys. Rev. B* **1986**, *33*, 8822.

(29) (a) Chang, C.; Pelissier, M.; Durand, P. *Phys. Scr.* **1986**, *34*, 394. (b) Heully, J.-L.; Lindgren, I.; Lindroth, E.; Lundquist, S.; Martensson-Pendrill, A. M. *J. Phys. B* **1986**, *19*, 2799. (c) Van Lenthe, E.; Baerends, E. J.; Snijders, J. G. *J. Chem. Phys.* **1993**, *99*, 4597. (d) Van Lenthe, E.; Baerends, E. J.; Snijders, J. G. *J. Chem. Phys.* **1996**, *105*, 6505. (e) Van Lenthe, E.; Van Leeuven, R.; Baerends, E. J.; Snijders, J. G. *Int. J. Quantum. Chem.* **1996**, *57*, 281. (f) Van Lenthe, E.; Ehlers, A. E.; Baerends, E. J. *J. Chem. Phys.* **1999**, *110*, 8943.

(30) Snijders, J. G.; Baerends, E. J.; Vernooijs, P. *At. Data Nucl. Tables* **1982**, *26*, 483.

(31) Baerends, E. J.; Ellis, D. E.; Ros, P. *Chem. Phys.* **1973**, *2*, 41.

(32) Krijn, J. G.; Baerends, E. J. *Fit Functions in the HFS-Method*; Internal Report (in Dutch); Vrije Universiteit Amsterdam: Amsterdam, The Netherlands, 1984.

(33) The exponents and coefficients of the ADF basis sets used are available on the following web pages: http://www.scm.com/Doc/atomicdata/ZORA/XXX with XXX = III/H for H, III/C.1s for C, III/O.1s for O, and IV/Re.4d for Re.

(34) (a) Fonseca Guerra, C.; Snijders, J. G.; Te Felde, G.; Baerends, E. J. *Theor. Chem. Acc.* **1998**, *99*, 391. (b) Bickelhaupt, F. M.; Baerends, E. J. In *Reviews in Computational Chemistry*; Lipkowitz, K. B., Boyd, D. B., Eds.; Wiley-VCH: New York, 2000, Vol. 15, p 1.

(35) Reed, A. E.; Curtiss, L. A.; Weinhold, F. *Chem. Rev.* **1988**, *88*, 899.

(36) (a) Dewar, J. S. *Bull. Soc. Chim. Fr.* **1951**, *18*, c71. (b) Chatt, J.; Duncanson, L. A. *J. Chem. Soc.* **1953**, 2939.

(37) (a) Dapprich, S.; Frenking, G. *Angew. Chem.* **1995**, *107*, 383; *Angew. Chem., Int. Ed. Engl.* **1995**, *34*, 354. (b) Pidun, U.; Frenking, G. *Organometallics* **1995**, *14*, 5325. (c) Pidun, U.; Boehme, C.; Frenking, G. *Angew. Chem., Int Ed. Engl.* **1996**, *35*, 2817. (d) Ehlers, A. W.; Dapprich, S.; Vyboishchikov, S. F.; Frenking, G. *Organometallics* **1996**, *15*, 105. (e) Dapprich, S.; Frenking, G. *Organometallics* **1996**, *15*, 4547. (f) Pidun, U.; Frenking, G. *J. Organomet. Chem.* **1996**, *525*, 269. (g) Frenking, G.; Pidun, U. *J. Chem. Soc., Dalton Trans.* **1997**, 1653. (h) Vyboishchikov, S. F.; Frenking, G. *Chem. Eur. J.* **1998**, *4*, 1428. (i) Vyboishchikov, S. F.; Frenking, G. *Chem. Eur. J.* **1998**, *4*, 1439. (j) Deubel, D. V.; Sundermeyer, J.; Frenking, G. *Inorg. Chem.* **2000**, *39*, 2314.

(38) (a) Deubel, D. V.; Sundermeyer, J.; Frenking, G. *J. Am. Chem. Soc.* **2000**, *122*, 10101. (b) Deubel, D. V.; Frenking, G.; Senn, H. M.; Sundermeyer, J. *Chem. Commun.* **2000**, 2469. (c) Deubel, D. V. *J. Org. Chem.* **2001**, *66*, 3790.

(39) Frisch, M. J.; Trucks, G. W.; Schlegel, H. B.; Scuseria, G. E.; Robb, M. A.; Cheeseman, J. R.; Zakrzewski, V. G.; Montgomery, J. A.; Stratmann, R. E.; Burant, J. C.; Dapprich, S.; Milliam, J. M.; Daniels, A. D.; Kudin, K. N.; Strain, M. C.; Farkas, O.; Tomasi, J.; Barone, V.; Cossi, M.; Cammi, R.; Mennucci, B.; Pomelli, C.; Adamo, C.; Clifford, S.; Ochterski, J.; Petersson, G. A.; Ayala, P. Y.; Cui, Q.; Morokuma, K.; Malick, D. K.; Rabuck, A. D.; Raghavachari, K.; Foresman, J. B.; Cioslowski, J.; Ortiz, J. V.; Stefanov, B. B.; Liu, G.; Liashenko, A.; Piskorz, P.; Komaromi, I.; Gomberts, R.; Martin, R. L.; Fox, D. J.; Keith, T. A.; Al-Laham, M. A.; Peng, C. Y.; Nanayakkara, A.; Gonzalez, C.; Challacombe, M.; Gill, P. M. W.; Johnson, B. G.; Chen, W.; Wong, M. W.; Andres, J. L.; Head-Gordon, M.; Replogle, E. S.; Pople, J. A. *Gaussian 98*, Revision A.3; Gaussian Inc.: Pittsburgh, PA, 1998.

(40) Dapprich, S.; Frenking, G. *CDA 2.1*; Universität Marburg: Marburg, Germany, 1994. The program is available via: ftp.chemie.uni-marburg.de/pub/cda.

(41) Frenking, G.; Antes, I.; Böhme, M.; Dapprich, S.; Ehlers, A. W.; Jonas, V.; Neuhaus, A.; Otto, M.; Stegmann, R.; Veldkamp, A.; Vyboishchikov, S. F. In *Reviews in Computational Chemistry*; Lipkowitz, K. B., Boyd, D. B., Eds.; VCH: New York, 1996; Vol. 8, p 63.

(42) We should emphasize the accuracy of the computational level at which this remarkable haptotropy has been predicted: (i) Computations give the same structures as those from X-ray crystallography; for instance, the calculated η^5 mode of the metal oxide and the η^3 mode of the diolate are in accordance with Herrmann's crystal structures (see ref 21). We have also found a good agreement between the results calculated using different basis sets and using different quantum-chemical program packages. (ii) The calculated η^1 structures were also obtained by geometry optimization using η^5-Cp systems as starting structures. (iii) The competition of the η^1 and η^5 coordination modes of Cp in the d^0-metal complexes MCp_4 with M = group 4 metals was recently studied experimentally and theoretically (Bursten, B. E. *INOR 378*, ACS Meeting, San Diego, April 1−5, 2001). $(\eta^1-Cp)_2(\eta^5-Cp)_2M$ (M = Ti, Hf) and $(\eta^1-Cp)_1(\eta^5-Cp)_3Zr$ structures were found. The DFT geometries calculated with ADF are in good agreement with X-ray structures. (iv) Note that allylic complexes of the type $RReO_3$ exhibit η^1 coordination rather than η^3, which was shown by NMR spectroscopy (Herrmann, W. A.; Kühn, F. E.; Romão, C. C.; Huy, H. T. *J. Organomet. Chem.* **1994**, *481*, 227), and that indenyltrioxorhenium-(VII) also exhibits η^1 coordination (Herrmann, W. A.; Kühn, F. E.; Romão, C. C. *J. Organomet. Chem.* **1995**, *489*, C56).

(43) Computational studies revealed that B3LYP is the superior functional for reactions of transition metal oxo and peroxo complexes: (a) Gisdakis, P.; Antonczak, S.; Rösch, N. *Organometallics* **1999**, *18*, 5044. (b) Deubel, D. V. *J. Phys. Chem. A* **2001**, *105*, 4765. The present work should therefore be considered a contribution toward a qualitative insight

into the origin of the activation energies rather than a report of quantitative data.

(44) Hammond, G. S. *J. Am. Chem. Soc.* **1955**, *77*, 334.

(45) (a) Bell, R. P. *Proc. R. Soc. London, Ser. A* **1936**, *154*, 414. (b) Evans, M. G.; Polanyi, M. *J. Chem. Soc., Faraday Trans.* **1936**, *32*, 1340.

(46) Fukui, K. *Acc. Chem. Res.* **1981**, *14*, 363.